

طريقة جديدة لتحديد المتغيرات على أساس النموذج التجريبي غير الخطي للاهتزازات الدوامية المستحدثة

جينغوين يان*، شياوشيا تيان* وتشى تشو**

* كلية الهندسة، جامعة شانتو، شانتو، الصين

** فني مختبر المنشآت ونفق الرياح لمعهد التعليم العالي في قوانغدونغ، شانتو، الصين

الخلاصة

تتناول الورقة التعرف على معلمات نموذج سكانلان غير الخطية للاهتزازات التي يسببها دوامة (VIV) من الطوابق الجسر. على الرغم من أن الخوارزمية الجينية (GA) لديها قدرة بحث جيدة، لديها صعوبات في تحسين مشكلة متعددة المعلمة للحصول على نتائج مقبولة. خوارزمية ليفنبرغ-ماركاردت (LMA)، خوارزمية التحسين المستخدمة على نطاق واسع، تتأثر بشدة بالحالة الأولية. تم اقتراح طريقة تعريف جديدة (GALMA) على أساس (GA) و (LMA). اعتمد (GA) لتحقيق الشرط الأولي، والذي يستخدم تباعاً من قبل (LMA) لتحسين تحديد الهوية. من أجل التحقق من صحة المعلمات المحددة، تتم مقارنة البيانات التي أعيد بناؤها مع البيانات المقاسة فيما يتعلق التاريخ الزمني للقوة العمودية التي يسببها دوامة (VIVF)، ومكونات تردد (VIVF)، والتاريخ الزمني للاستجابة النزوح. وتظهر النتيجة (GALMA) فعالة. وعلاوة على ذلك، بالمقارنة مع أساليب أخرى محددة، (GALMA) هو أكثر دقة في تحديد المعلمات، وخاصة العديد من المعلمات من المعادلة.

A novel method of parameter identification based on nonlinear empirical model for vortex- induced vibration

Xiaoxia Tian*, Jingwen Yan** and Qi Zhou***

* College of Computer Science and Engineering, Hanshan Normal University, Chaozhou, China

** College of Engineering, Shantou University, Shantou, China

***Key Laboratory of Structure and Wind Tunnel of Guangdong Higher Education Institutes, Shantou, China

Corresponding author: 14xxtian@stu.edu.cn

ABSTRACT

The paper deals with the identification of the parameters of Scanlan's nonlinear model for the vortex-induced vibrations (VIV) of bridge decks. Although genetic algorithm (GA) has a good search ability, it has difficulties in optimizing the multi-parameter problem to obtain acceptable results. Levenberg-Marquardt algorithm (LMA), a widely used optimization algorithm, is strongly influenced by the initial condition. A novel identification method (GALMA) based on GA and LMA has been proposed. GA is adopted to achieve an initial condition, which is successively used by LMA to optimize the identification. In order to verify the validity of the identified parameters, the reconstructed data is compared with the measured data with respect to the time history of vortex-induced vertical force (VIVF), the frequency components of VIVF, and the time history of displacement response. The result shows that GALMA is effective. Furthermore, compared with other identified methods, GALMA is more precise in identification parameters, especially many parameters of equation.

Keywords: Nonlinear least squares; vortex-induced vertical force; genetic algorithm; levenberg-marquardt algorithm.

INTRODUCTION

Vortex-induced Vibration (VIV) is one of the current hotspots that highlights the wind engineering. Among the bridge structures, long-span bridges, low damping, and large flexible, are the most susceptible to the wind (Ehsan, 1988; Gupta *et al.*, 1996; Scanlan, 1998; Marra *et al.*, 2011; Zhang *et al.*, 2014). Vortex-induced vibration generally occurs in certain wind speed when vortex -shedding frequency is close to the bridge natural frequency, and has the characteristics of self-limiting and self-excited.

Although VIV response does not directly result in the bridge catastrophic events, it causes the fatigue damage of the bridge and the reduction of service performance, such as travel safety and driving comfort. Whereas, many researchers (Birkhoff, 1953; Bishop & Hassan, 1964; Skop & Griffin, 1973; Sarpkaya, 1978; Scanlan, 1981; Dowell, 1981; Goswami *et al.*, 1993; D'Asdia *et al.*, 2003) have paid attention to the complex physical phenomenon in order to model a bridge deck against the vortex-induced vibration. But the physical mechanism of VIV is so intricate that it is not

possible to build the theoretical model. At present, it is a very effective way to establish the semi-empirical mathematical model based on careful observation on wind tests or actual phenomena. Although the semi-empirical mathematical model cannot fully exposit the mechanism of vortex-induced vibrations, it formulates the characteristics of the vortex-induced vibration phenomena, for instance, self-excited and self-limiting.

The semi-empirical mathematical models aim to predicting the body oscillation amplitude with the identified parameters at different values of wind speed, mass, and damping, but it is difficult to identify the parameters from experimental data according to complexity of the VIV system. Among those models, the empirical model of Signal-Degree-of-Freedom (SDoF) proposed by Scanlan (1981) is successfully applied to wind tunnel tests (Ehsan, 1988), and the model can describe the overall lock-in phenomenon. In the present work, the Scanlan's model, as a realistic case, is deeply studied.

For the Scanlan's nonlinear model, the parameter identification methods are divided into two categories. One class depends on the measured data of steady-state vibration, the Grow to Resonance (GTR) or the Decay to Resonance (DTR) (Ehsan & Scanlan, 1990) is perhaps the most general and easily applicable technique because the steady amplitude of the VIV displacement response can be directly measured in the test. The GTR does not work in the following cases: the steady-state amplitude is very small and cannot be observed with sufficient accuracy. In addition, ubiquitous noise also affects the accuracy of steady-state amplitudes. The other class, which is independent of the value of steady-state vibration, is based on least squares theory. Since there is no closed-form solution to a non-linear least squares problem, numerical algorithms are used to find the value of the parameters. Gupta *et al.* (1996) proposed an alternative identification based on the theory of invariant imbedding. Weng *et al.* (2014) proposed a method to identify the aero-elastic parameters from the time history of measured displacement, and they made use of the GA to get nonlinear fitting. Zhu *et al.* (2013) proposed a method to identify the aero-elastic parameters from the measured vortex-induced vertical force (VIVF) time histories and to employ Levenberg–Marquardt algorithm (LMA) to get the optimal solution. However, those algorithms are not perfect in solving the nonlinear problems. GA is liable to obtain local minimum in spite of its excellent search ability (Perry *et al.*, 2006; Toğan & Daloğlu, 2008). LMA can cope with the nonlinear problem, while it is sensitive to initial conditions (Gavin, 2011; Transtrum & Sethna, 2012). On account of the limitation of knowledge about the mechanism of vortex-induced vibration, it is difficult to obtain the appropriate initial conditions corresponding to the global optimum.

In addition, new models based on Scanlan's nonlinear model have been proposed. Marra *et al.* (2015) found that the relation between the Scruton number and the linear, damping coefficient of Scanlan's model is linear and the relation between the Scruton number and the nonlinear damping coefficient is quadratic. So the parameters are identified by three decay -to- resonance tests for three different Scruton numbers. Wu & Kareem (2013) presented a model based on Volterra series, the simplified Scanlan's model plays an important role in the identification of parameters. Mashnad & Jones. (2014) put forward a model similar to Scanlan's nonlinear model, they extracted aero-elastic damping coefficient and stiffness coefficient from wind tunnel tests at several wind speeds. In these models, the envelope of a decaying or growing displacement is used to identify

the parameters, thus, the accuracy of measured displacement directly affects the reliability of identification results. The displacement on the sectional model is very small, it is therefore difficult to measure displacement with high accuracy in the conventional sectional model test. What's more, the reliability of these models and its parameter identification methods need to be further verified. So the Scanlan's nonlinear model is used to analyses vortex-induced resonance (VIR) system in this paper, a GALMA method based on optimization theory is proposed to identify parameters from wind tunnel test, it can search for an appropriate initial condition, and achieve the optimal solution of the parameters.

The rest of the paper is organized as follows. In Section 2, a brief introduction of the Scanlan's model is given, then the nonlinear optimization based on least squares theory is mainly discussed. In Section 3, the detailed information of the GALMA method is presented. In Section 4, the parameters are identified from the wind tunnel test, then the validity of the parameters is verified through the time history of VIVF, frequency components, and displacement of bluff body. Then The results of different identification methods are analyzed. Section 5 summarizes the paper.

RELATED WORKS OF IDENTIFICATION PARAMETERS

In this section, the nonlinear empirical model of the SDoF and the traditional identification method are described in brief. Then nonlinear optimization based on least squares theory is presented in detail.

Nonlinear empirical model of SDoF

In terms of velocity and displacement, the VIVF, which acts on the bluff model under lock-in condition, mainly contains a harmonic component and nonlinear component. These two components are caused by vortex shedding and aero-elastic interaction acting on bluff body and air flow, respectively. According to the nonlinear empirical model proposed by Ehsan and Scanlan (1990), the equation of motion in the cross-flow degree-of-freedom y can be written as follows.

$$m[y + 2\xi\omega_0\dot{y} + \omega_0^2 y] = f_v(y, \dot{y}, U, t) \quad (1)$$

Where m is the mass of the bridge deck per unit length; ω_0 is the natural frequency of the bridge at zero wind speed; ξ is the mechanical damping ratio; U is the velocity of the oncoming flow; f_v is the aerodynamic force per unit length due to the vortex shedding, which is a function of wind velocity U , displacement y , velocity \dot{y} , and time t of the sectional model vibration.

$$f_v(y, \dot{y}, U, t) = \frac{1}{2} \rho U^2 D \left[Y_1 \left(1 - \varepsilon \frac{y^2}{D^2} \right) \frac{\dot{y}}{U} + Y_2 \frac{y}{D} + \frac{1}{2} C_L \sin(\omega_{vs} t + \psi) \right] \quad (2)$$

Where ρ is the air density; D is the depth of the bridge deck; ω_{vs} is the circular oscillation frequency in the case of vortex-induced resonance; y and \dot{y} are the oscillating displacement and velocity of the bluff bridge deck, respectively; ψ is the phase angle; Y_1 is the linear aero-elastic damping; Y_2 is the linear aero-elastic stiffness; ε is the nonlinear aero-elastic damping; C_L is the sinusoidal approximation of the fluctuating lift coefficient; ω_{vs} is the mechanical circular frequency during VIV.

In the paper, the vertical vortex-induced force (VIVF) is analyzed. So the dimensionless motion equation of VIVF can be expressed as follows.

$$\eta''(s) + 2\xi K_0 \eta'(s) + K_0^2 \eta(s) = \tilde{f}_{Vf} \quad (3)$$

$$\tilde{f}_{Vf} = m_r \left[Y_1 (1 - \varepsilon \eta(s)^2) \eta'(s) + Y_2 \eta(s) + \frac{1}{2} C_L \sin(K_{vs} s + \psi) \right] \quad (4)$$

Where $m_r = \rho D^2 / m$; $K_0 = \omega_0 D/U$; $K_{vs} = \omega_{vs} D/U$ is the circular oscillation frequency in the case of vortex-induced resonance; $s = tU/D$ is the dimensionless time; $\eta(s) = y(t)/D$ is the dimensionless displacement; $\eta'(s) = \dot{y}(t)/U$ is the dimensionless velocity; \tilde{f}_{Vf} is the dimensionless VIVF.

Nonlinear optimization based on least squares theory

The model parameters are identified by the nonlinear least squares from the time history of measured VIVF. The objective function is defined as follows:

$$R(Y_1, Y_2, \varepsilon, C_L, K_{vs}, \psi) = \frac{1}{2} \sum_{i=1}^N (\tilde{f}_{Vf}(s_i) - \hat{f}_{Vf}(s_i))^2 \quad (5)$$

Where $\tilde{f}_{Vf}(s_i)$ and $\hat{f}_{Vf}(s_i)$ are the values of the dimensionless VIVF at the dimensionless time s_i measured in the test and reconstructed by Eq. , respectively; N is the total number of the data points of the \tilde{f}_{Vf} samples.

Let $x = (Y_1, Y_2, \varepsilon, C_L, K_{vs}, \psi)^T$ be viewed as a vector. If x_+ is a global minimizer of function $R(x)$, The least squares method for the problem can be expressed as follows.

$$x_+ = \arg \min_{x \in R^6} \{R\} \quad (6)$$

The Eq. is in itself an unconstrained optimization problem, which is hard to solve generally. It is relatively easy for the local optimal x^* to be obtained.

$$R(x^*) \leq R(x) \quad \text{for} \quad \|x - x^*\| < \varepsilon \quad (7)$$

Where ε is a small positive number, the local optimal x^* must satisfy the conditions $\nabla R(x^*)=0$ and $h^T \nabla^2 R(x^*) h > 0$. is a nonzero vector.

Genetic algorithms

Genetic algorithms are commonly used to generate high-quality solutions to optimization and search problems by relying on bio-inspired operators such as mutation, crossover, and selection.

GA has a well-known disadvantage that the solutions may converge to local optima, and may find difficulty to escaping to find the global optimum solution. Perry *et. al.* (2006) modified classical GA strategy to identify unknown parameters such as mass, stiffness, and damping properties of a structure system. The strategy includes multiple populations and, a search space reduction procedure and so on. Crossover and mutation are the key to affect the behavior and performance of GA.

The iterative process starts from a population of randomly generated individuals in a given range. In each iterative, the fitness of every individual in the population is evaluated. the fitness is the value of the objective function . According to a predetermined rule, some individuals may be selected, mutated, or altered to form a new population. The new population is then used in the

next iteration of the algorithm. The algorithm terminates when a maximum number of iterative has been produced. Finally, the output is an individual with the smallest fitness value is selected from the latest population.

Levenberg-marquardt algorithm (LMA)

LMA relies on the basic concepts of optimization theory (Gavin, 2011; Dkhichi *et al.*, 2014; Transtrum & Sethna, 2012). It merges the steepest descent method with the concept of minimizing the Taylor approximation of the function . As for Eq. , it is satisfied $\nabla R(x^*) = 0$, so this is a nonlinear system of equations, and it forms the Taylor expansion.

$$\begin{aligned} \nabla R(x+h) &= \nabla R(x) + \nabla^2 R(x)h + \text{higher order terms of } h \\ &; \nabla R(x) + \nabla^2 R(x)h \quad \text{for } \|h\| \text{ sufficiently small} \end{aligned} \quad (8)$$

The gradient matrix and the hessian matrix of the objective function $R(x)$ can be expressed as follows, respectively.

$$\begin{aligned} \nabla R(x) &= J(x)^T R(x) = \sum_{i=1}^n R_i(x) \nabla R_i(x) \\ H(x) &= \nabla^2 R(x) = \sum_{i=1}^n \nabla R_i(x) (\nabla R_i(x))^T + \sum_{i=1}^n R_i(x) \nabla^2 R_i(x) \\ &= J(x)^T J(x) + S(x) \end{aligned}$$

Where $J(x) = \nabla R(x)$ is the Jacobian matrix, $S(x) = \sum_{i=1}^n R_i(x) \nabla^2 R_i(x)$. If $\nabla^2 R_i(x)$ or $R_i(x)$ is small, the Hessian matrix in this case simply becomes

$$H(x) = \nabla^2 R(x) = J(x)^T J(x)$$

So the update rule of LMA is given as:

$$x_{i+1} = x_i + d_i \quad (9)$$

$$d_i = -(H + \lambda I)^{-1} \nabla R(x_i) \quad (10)$$

The essence of the LMA is a linear approximation to $R(x)$ in the neighborhood of x . For all $\lambda \geq 0$ the coefficient matrix is positive definite, and this ensures that d_i is a descent direction. if λ is small, which is a good step in the final stages of the iteration, when x is close to x^* , the direction d_i is identical to that of the Gauss-Newton method. While λ is large, d_i tends to the steepest descent direction, with magnitude tending to zero. Therefore, it is to guarantee the convergence of function $R(x)$ that the term λ can adaptively controls both the direction and the size of the step.

The LMA has repeatedly updated Eq. and Eq. until the acceptable solution is found. The stopping criteria of the iteration are written as follows.

1) The solution can be achieved when $\nabla R(x^*) = 0$, the algorithm terminates.

$\|\nabla R(x)\|_{\infty} < \varepsilon_1$, where ε_1 is an any small, positive specified number.

2) If the current iteration number k is greater than the maximum number of iterations k_{\max} , the algorithm terminates.

THE GALMA METHOD FOR IDENTIFICATION PARAMETERS

The GALMA method proposed in this paper is based on the least squares theory. It can adopt GA to generate the appropriate initial condition, which is successively used by LMA to optimize the identification. The method, therefore, mainly contains GA and LMA.

The GA module generates the initial vector ini_x with respect to Eq. . The genetic algorithm randomly selects 500 individuals from the predetermined range $[6, 10; -12, -18; 0, -3; 0, 1; 0.4, 0.8; 0, 6]$ to form a population . The GA starts an iterative process with the population. In each iteration, the fitness of every individual in the population is evaluated, the individuals are selected from the current population according to the selection probability $ps = 95\%$, and some individual's genome is modified to form a new population $P_{new} = (x'_1, x'_2, \dots, x'_{500})$. The new population of candidate solutions are then used in the next iteration of the algorithm. the algorithm terminates when a satisfactory fitness level or the maximum number of iterations has been reached.

The Genetic Algorithm

<p>Input: A fitness function f , $\varepsilon = 1e-10$ is the limit error, initial range $range = [6, 10; -12, -18; 0, -3; 0, 1; 0.4, 0.8; 0, 6]$, the number of population P is 500, and the maximum number of iterations $k_{max} = 1000$</p>
<p>Output: ini_x is a solution</p>
<p>Step 1 : $k = 0$ Step 2 : $ps = 0.95\%$ Selection probability Step 3 : $pc = 0.8; pm = 0.08\%$ crossover and mutation probabilities Step 4 : $p(k)\%$ randomly generate the population within the initial range Step 5 : $Objv = f(p(k))\%$ the value of each individual in $p(k)$ is calculated by Eq. Step 6 : <i>while</i> $k < k_{max}$ Step 7 : $k = k + 1$; Step 8 : $Fitnv = rank(Objv)\%$ the fitness value of each individual is evaluated</p>
<p>Step 9 : $temp = select(p(k-1), Fitnv, ps)\%$ selection Step 10: $temp = crossover(temp, Fitnv, pc)\%$ crossover and mutation Step 11: $p(k) = mutation(temp, Fitnv, pm)\%$ mutation Step 12: $Objv = f(p(k))$ Step 13: <i>end</i> Step 14: $ini_x = find(p, \min(Objv))\%$ select an individual with the smallest fitness Step 15: <i>output</i> ini_x</p>

In the LMA module, an initial parameter vector ini_x and a measured VIVF are provided, the LMA searches for an optimal solution in the neighborhood of ini_x . The detailed description of the algorithm is as follows.

The Levenberg- Marquart Algorithm

Input: A function $f(x)$, a measured VIVF vector $f_{measure}$ an initial parameter ini_x , $\varepsilon_1=1e-6$ is the limit error, step factor $\lambda=0.005$ and the maximum number of iterations $k_{max}=100$.

Output : x is the optimal

Step 1 : $k = 0$; $x = ini_x$; $updateJ = 1$; $g = 1$

Step 2 : *while* $\|g\| > \varepsilon_1$ *and* $k < k_{max}$

Step 3 : $k = k + 1$;

Step 4 : *if* $updated == 1$

Step 5 : $g = \nabla f(x)$; $H = J(x)^T J(x)$ %compute the Jacobin and gradient

Step 6 : *if* $k == 1$

Step 7 : $sumq = sum((f(x) - f_{measure})^2)$ %compute sum of squares

Step 8 : *endif*

Step 9 : *endif*

Step 10: $d = -(H + \lambda diag(H))^{-1} g$ %compute LMA step

Step 11: $x_{temp} = x + d$ %update x with reconstructed step

Step 12: $sumq_{temp} = sum((f(x_{temp}) - f_{measure})^2)$ %updated sum of squares

Step 13: *if* $sumq_{temp} < sumq$ % if the sum squared error has been reduced

Step 14: $x = x_{temp}$ % update x

Step 15: $sumq = sumq_{temp}$ % update sum of squares after convergence test

Step 16: $\lambda = \lambda / 10$; $updateJ = 1$ % reduce λ , only the previous step is good

Step 17: *else*

Step 18: $\lambda = \lambda * 10$ %increase LMA parameter

Step 19: $updateJ = 0$ %unsuccessful step, no need to re-compute the Jacobian

Step 20: *endif*

Step 21: *end*

Where $sumq$ is named the sum of squares between the reconstructed VIVF and the measured VIVF about x . If $sumq_{new} < sumq$, the parameter vector x is replaced by a new estimated $x + d$ where the direction d is calculated using Eq. $sumq_{new} \geq sumq$, and the parameter is λ reduced. If , the parameter λ is increased.

NUMERICAL SIMULATION

Any new method needs to be tested numerically in order to evaluate its performance in an experimental situation. A series of tests have been carried out in TJ-3 boundary layer wind tunnel of the state Key Laboratory for Disaster Reduction in Civil Engineering at Tongji university. While the Simulation environment includes software and hardware as follows:

Software: windows 10 is the operating system; MATLAB 2010b is the development software.

Hardware: Intel(R) core(TM) i5-3470 CPU@ 3.2GHZ; RAM 4.0GB.

The simulation result of GALMA method

In the GA module, the number of population is finely set to 500; the selection, crossover, and mutation probabilities is 0.95, 0.8, and 0.08, respectively; the maximum number of iterations is 1000. The solution is [7.8339 -17.0669 -2.3235 0.7000 0.6800 2.8000]. The sum of squares for error (SSE) and coefficient of determination (R-square) of GA is 0.0022 and 0.5697, respectively.

In the LMA module, the threshold of first-order optimality is set to 1e-6, the initial Lambda $\lambda=0.001$ and the maximum number of iterations $k_{max} = 100$ are specified. With the initial condition from GA, LMA goes through 17 iterations to obtain the optimal solution. Table 1 shows the results of each iteration, including iteration, residual, first order optimality, and lambda. The algorithm stops because the first-order optimality, 5.54e-006, is less than 1e-6. The optimal is [8.240 -2.1911 -14.484 0.6327 0.6797 4.083]. Its SSE and R-square is 0.0019 and 0.6291, respectively.

Table 1. The output of each iteration.

Iteration	Residual	First-Order optimality	Lambda
0	0.0022321	1.4	0.001
1	0.00206895	0.0379	0.0001
2	0.00198958	0.0665	1e-005
3	0.00193898	0.0313	1e-006
4	0.00192726	0.0165	1e-007
5	0.00192476	0.00756	1e-008
6	0.0019241	0.00379	1e-009
7	0.00192396	0.0018	1e-010
8	0.00192393	0.00088	1e-011
9	0.00192393	0.000426	1e-012
10	0.00192393	0.000208	1e-013
11	0.00192393	0.000101	1e-014
12	0.00192393	4.91e-005	1e-015
13	0.00192393	2.39e-005	2.22045e-016
14	0.00192393	1.16e-005	2.22045e-016
15	0.00192393	5.54e-006	2.22045e-016
16	0.00192393	7.2e-007	0.000222045

The reliability and accuracy of the identified parameters have been checked with respect to different aspects. Firstly, the VIVF response, which is reconstructed by Eq. with the identified parameters, is well consistent with to the measured one, as shown in Figure 2 (d). Secondly, Figure 3 (d) shows that the reconstructed VIVF and the measured VIVF have the same frequency components, which are 2.814Hz, 5.627hz, and 8.441hz, respectively. Thirdly, the reconstructed displacement time history has been compared with the measured one, as shown in Figure 1. It can

be found that the reconstructed displacement response and the measured displacement response agree well with each other, this indicates that the GALMA method in this study is effective.

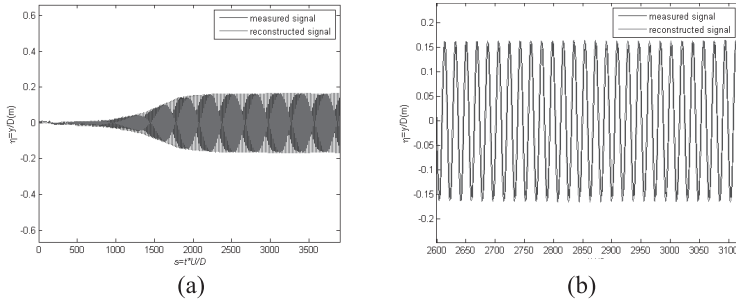


Figure 1. The measured displacement and the reconstructed one with identified parameters at $\xi=0.5\%$ and $U = 9.1\text{m/s}$. The parameters of Newmark- β method are set to $\alpha=0.6$ and $\beta=0.25$.

(a) Overall view;

(b) partial view.

Analysis of the simulation results of different methods

These methods, which consists of GTR, LMA (Zhu *et al.*, 2013), GA, and GALMA, have been adopted to identify the parameters of the Scanlan's model in the paper. The estimated parameters $Y_1, Y_2, \varepsilon, C_L, \omega_s, \psi$ shown in Table 2 were extracted from the experimental data with a nominal damping ratio ξ of 0.5% and a wind speed (U) of 9.1m/s. The results of GTR and LMA comes from the literature (Zhu *et al.*, 2013).

Table 2. Identification parameters from different methods.

method	Y_1	Y_2	ε	C_L	ω_s	ψ
GTR	16.397	-0.641	81.199			
LMA	8.406	-2.179	-18.671	0.792	0.680	-1.997
GA	7.8339	-2.3235	-17.0669	0.701	0.680	2.800
GALMA	8.240	-2.1911	-14.484	0.6327	0.6797	4.083

The fitting evaluation parameters of the four methods, including SSE, mean square error (MSE), root mean squared error (RMSE), and R-square, are shown in the Table 3. The R-square is the key for the result of fitting. The closer to 1 R-square is, the more ideal is the fitting. The SSE is the secondary judgment. The smaller the SSE is, the smaller the error between the measured VIVF and the reconstructed results is. The same is true for MSE and RMSE.

Table 3. Error parameter comparison of different identified methods.

Method	SSE	MSE	RMSE	R-square
GTR	0.0014	4.6934e-008	2.1664e-004	0.1762
LMA	0.0042	1.3633e-007	3.6922e-004	0.1931
GA	0.0022	7.2704e-008	2.6964e-004	0.5697
GALMA	0.0019	6.2667e-008	2.5033e-004	0.6291

There are several figures that can clarify the performance of the above four methods. Figure 3 shows the time history of the measured VIVF is compared with that of the VIVF reconstructed by different methods. And it can be seen that there are significant differences between the measured time history of VIVF and the reconstructed one in both the curve pattern and the magnitudes. From Figure 2 (a), The reconstructed VIVF curve has three positive peaks within one period, while the measured VIVF curve has only two positive peaks. The reconstructed VIVF curve in Figure 2 (b) has two positive peaks in a period. One is high, while the other is low. The reconstructed VIVF curve in Figure 3 also has two positive peaks in a period. The left peak is apparent higher than the right peak. As far as Figure 2 (d) is concerned, the reconstructed VIVF has two almost same peaks in a period. What's more, Figure 3 shows the frequency components of the different signals. There are three main peaks in the amplitude spectra of the measured VIVF, in other words, it has three main frequency components, which are 2.814Hz, 5.627Hz, and 8.441Hz, respectively. The VIVF reconstructed by GTR has only two frequency components: 2.814Hz and 8.441Hz, shown in Figure 3 (a), while the VIVFs reconstructed by the other methods have the same frequency components as the measured one has.

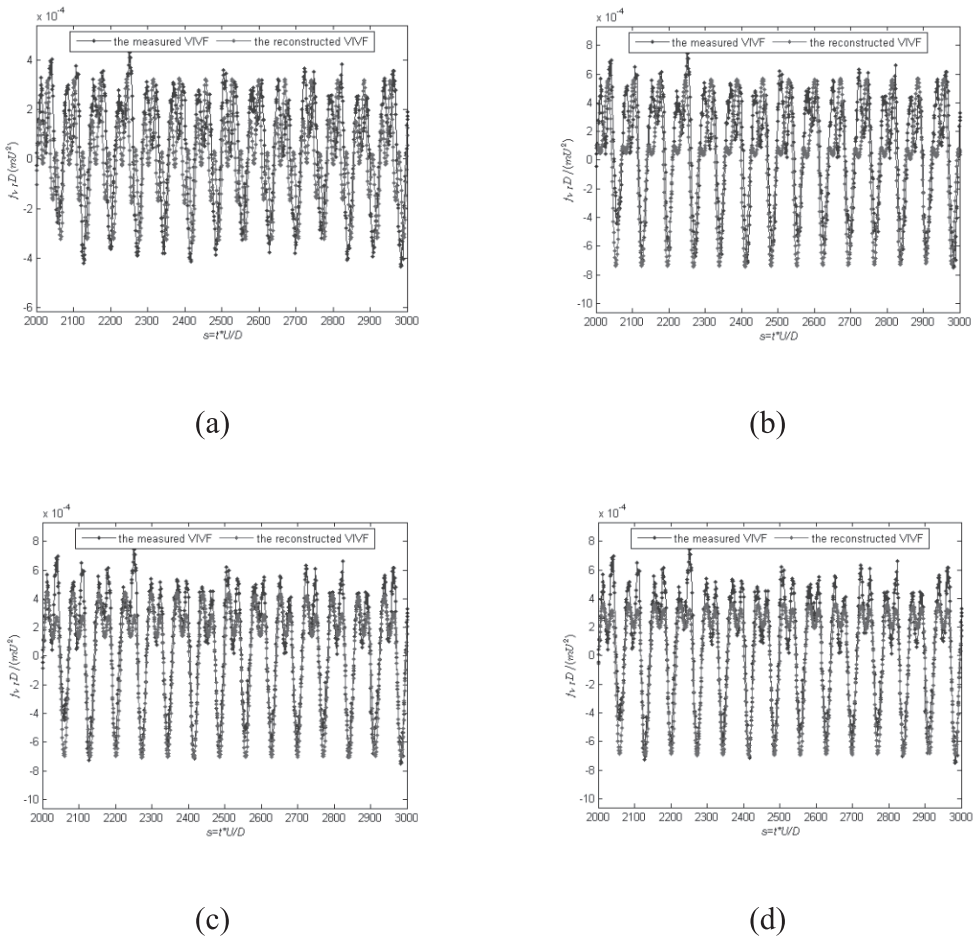


Figure 2. The dimensionless reconstructed VIVF with different methods compared with the measured one at $U = 9.1$ and $\xi=0.5\%$. (a) GTR; (b) LMA; (c) GA; (d) GALMA.

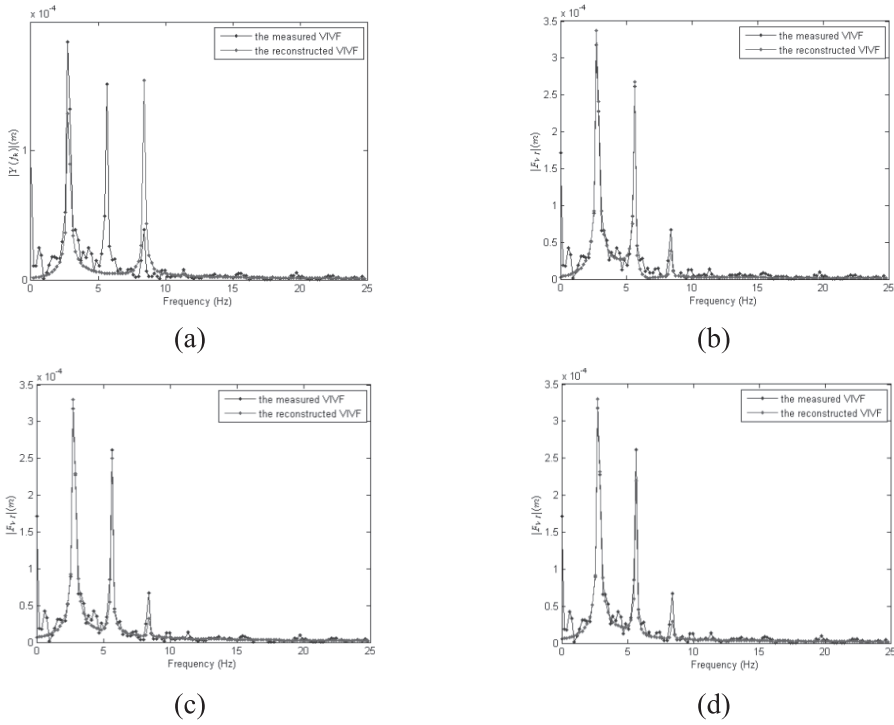


Figure 3. The contrast diagram of the amplitude spectra of the measured VIVF and the reconstructed VIVF at $U = 9.1$ and $\xi = 0.5\%$. (a) GTR; (b) LMA; (c) GA; (d) GALMA.

From the Table 3, SSE and R-square of the GTR method are 0.0014 and 0.1762, respectively. Its SSE is the smallest because of a closed-loop process from the parameters identification to the parameters verification. The parameters of an uncertain vibration model have been extracted from the displacement responses in the wind tunnel, then those identified parameters have been used to reconstruct the displacement responses with the same model, the validity of the identical parameters is verified by comparing the measured displacement with the reconstructed displacement. Moreover, the distortion caused by the vibration model can be automatically eliminated in the whole process. In terms of the R-square, the GTR is the worst. The reason of this phenomenon is that the main component frequency of the measured VIVF are not the same as that of the reconstructed VIVF. The Figure 2 (a) shows significant differences between the measured and the reconstructed time histories of VIVF in both curve pattern and magnitude. There are three positive peaks in one cycle of the GTR, but only two positive peaks in a period of the measured VIVF. From Figure 3 (a), three main frequencies in the time history of the measured VIVF are 2.81Hz, 5.62Hz, and 8.4Hz, but the time history of the VIVF reconstructed by GTR has two main, frequencies 2.81Hz and 8.4Hz.

Those methods, including GA, and LMA, have three frequency spectra and two positive peaks within a period of time history of the reconstructed VIVF. However, there are significant differences in the magnitudes of VIVF spectra shown in Figures 3 (b) and 3 (c). In Table 3, SSE and R-square of LMA method are 0.0042 and 0.1931, respectively. While SSE and R-square of GA are 0.0022 and 0.5697, respectively. In total, GA demonstrates its outstanding search capabilities perfectly, and LMA does not do well because of an inappropriate initial.

For GALMA, its SSE and R-square are 0.0019 and 0.6291, respectively. GALMA with the advantage of GA and LMA is superior to LMA due to the following aspects. One is that the appropriate vector corresponding to the optimal is regarded as the initial, another is the parameter λ that is not a constant in order to obtain the optimal fast. Among the four methods, the GALMA has the minimum error and the maximum R-square, and the parameters identified by GALMA is the most accurate description about the response of the prototype.

CONCLUSION

The nonlinear least squares theory is applied in GALMA. the parameters identified by GALMA have been verified to be accurate, and explain the phenomenon of vortex shedding for flat closed box deck. Its advantages are summarized as follows:

- GALMA achieves the optimal solution quickly and accurately. GA is employed to search for a solution, which is regarded as the initial parameters of LMA. LMA can use the finite difference to get the Jacobin matrix and adaptively adjust the parameter λ in order to obtain the optimal solution rapidly.
- The validity of parameters has been verified successfully. Firstly, the time history of VIVF reconstructed by Eq. with identified parameters agrees well with that of the measured VIVF, because they have similar frequency spectra. Secondly, the reconstructed displacement response of the sectional model at the different damping ratio also agrees well with the measured one.
- Four methods of identification parameters (GTR, LMA, GA, and GALMA) are compared in terms of fitting evaluation parameters, the time history of VIVF, the frequency spectra of VIVF, and the displacement responses of sectional model at the damping ratios ξ of 0.5% and 0.7%, respectively. The reconstructed VIVF has only two frequency spectra, which results in a great difference to the measured VIVF. So it can be found from Table 3 that the R-square of the GTR method is merely 0.1762. Although LMA and GA improve the value of R-square describing the equality of a fit, and contain three frequency spectra, their R-square is 0.1931 and 0.5697, respectively,. While the R-square of GALMA is 0.6291, considering the effect of fitting, GALMA is superior to other methods.

However, there are several problems in the processing of identified parameters. Firstly, as for the measured data, it can be seen from Figure 3 that the amplitude in the around 0 frequency is not equal to 0, which means that the vortex-induced force mathematical model must include a constant term, but Scanlan's empirical nonlinear model does have not a constant term. Secondly, the parameter k_{vs} reaches 0.68, 2 times of the major reduced frequency of the vortex-induced vibration, which is abnormal. Thirdly, the coefficient Y_2 usually is very small in air, but it is positive since the flow around the oscillating body tends to increase the oscillating mass and then to reduce the oscillation frequency. Conversely, the value provided by GALMA is negative. In addition, the parameter ε regulates the oscillation amplitude at zero structural damping, and its value should be positive instead of the negative value obtained.

The proposed method aims to at identifying the parameters of Scanlan's nonlinear model from the measured data. While we found that the identified parameters could not explain the physical

mechanism of VIR very well. From the previous analysis, it can be found that the measured data contains harmonic and high frequency components, while the Scanlan's nonlinear model does not include those components. Therefore, a new model of VIR, including harmonic and high-frequency components, is the direction of our next research.

ACKNOWLEDGEMENTS

The writers authors are grateful to Wei Huang Ph. D., Ruyi Feng Ph. D., and other reviewers of the original manuscript of the paper, who give helpful suggestions and comments. This paper is supported by the State Natural Science Fund project of China (51308330) and by the 2015 open fund of Structure and wind tunnel key laboratory of Guangdong Province (201502).

REFERENCES

- Birkhoff G. 1953.** Formation of vortex streets. *Journal of Applied Physics*, **24**(1): 98-103.
- Bishop, R. E. D. & Hassan, A. Y. 1964.** The lift and drag forces on a circular cylinder oscillating in a flowing fluid. *Proceedings of the Royal Society of London A: Mathematical, Physical and Engineering Sciences*. The Royal Society, **277**(1368): 51-75.
- D'Asdia, P., Sepe, V., Caracoglia, L. & Noè, S. 2003.** A model for vortex-shedding induced oscillations of long-span bridges. *Proceedings of the 2nd International Structural Engineering and Construction Conference (ISEC-02)*. **3**: 2331-2336.
- Dkhichi, F., Oukarfi, B., Fakkar, A. & Belbounaguia, N. 2014.** Parameter identification of solar cell model using Levenberg–Marquardt algorithm combined with simulated annealing. *Solar Energy*, **110**:781-788.
- Dowell E. H. 1981.** Non-linear oscillator models in bluff body aero-elasticity. *Journal of Sound and Vibration*, **75**(2): 251-264.
- Ehsan F. 1988.** The vortex-induced response of long, suspended-span bridges.
- Ehsan, F. & Scanlan, R. H. 1990.** Vortex-Induced Vibrations of Flexible Bridges. *Journal of Engineering Mechanics*, **116**(6):1392-1411.
- Gavin, H. 2011.** The Levenberg-Marquardt method for nonlinear least squares curve-fitting problems.
- Goswami, I., Scanlan, R. H. & Jones, N. P. 1993.** Vortex-induced vibration of circular cylinders. I: experimental data. *Journal of Engineering Mechanics*, **119**(11): 2270-2287.
- Gupta, H., Sarkar, P. P. & Mehta, K. C. 1996.** Identification of vortex-induced-response parameters in time domain. *Journal of Engineering Mechanics*, **122**(11): 1031-1037.
- Marra, A. M., Mannini, C. & Bartoli, G. 2011.** Van der Pol-type equation for modeling vortex-induced oscillations of bridge decks. *Journal of Wind Engineering and Industrial Aerodynamics*, **99**(6): 776-785.
- Marra, A. M., Mannini, C. & Bartoli, G. 2015.** Measurements and improved model of vortex-induced vibration for an elongated rectangular cylinder. *Journal of Wind Engineering and Industrial Aerodynamics*, **147**:358-367.
- Mashnad, M. & Jones, N. P. 2014.** A model for vortex-induced vibration analysis of long-span bridges. *Journal of Wind Engineering and Industrial Aerodynamics*, **134**: 96-108.
- Perry, M. J., Koh, C. G. & Choo, Y. S. 2006.** Modified genetic algorithm strategy for structural identification. *Computers & Structures*, **84**(8): 529-540.
- Sarpkaya, T. 1978.** Fluid forces on oscillating cylinders. NASA STI/Recon Technical Report A, **78**: 46523.

- Scanlan, R. H. 1981.** State-of-the-art methods for calculating flutter, vortex-induced, and buffeting response of bridge structures. No. FHWA-RD-80-50 Final Rpt.
- Scanlan, R. H. 1998.** Bridge flutter derivatives at vortex lock-in. *Journal of Structural Engineering*, **124**(4): 450-458.
- Skop, R. A. & Griffin, O. M. 1973.** A model for the vortex-excited resonant response of bluff cylinders. *Journal of Sound and Vibration*, **27**(2): 225-233.
- Toğan, V. & Daloğlu, A. T. 2008.** An improved genetic algorithm with initial population strategy and self-adaptive member grouping. *Computers & Structures*, **86**(11): 1204-1218.
- Transtrum, M. K. & Sethna, J. P. 2012.** Improvements to the Levenberg-Marquardt algorithm for nonlinear least-squares minimization. arXiv preprint arXiv:1201.5885.
- Weng, X. Y., Yao-Jun, G. E. & Chen, H. X. 2014.** New approach for identifying aerodynamic parameters in nonlinear vortex induced force model. *Zhendong Yu Chongji/journal of Vibration & Shock*, **33**(6):82-65.
- Wu, T. & Kareem, A. 2013.** Vortex-induced vibration of bridge decks: Volterra series-based model. *Journal of Engineering Mechanics*, **139**(12): 1831-1843.
- Zhang, Z., Ge, Y. & Chen, Z. 2014.** Vortex-induced oscillations of bridges: theoretical linkages between sectional model tests and full bridge responses. *WIND AND STRUCTURES*, **19**(3): 233-247.
- Zhu, L. D., Meng, X. L. & Guo, Z. S. 2013.** Nonlinear mathematical model of vortex-induced vertical force on a flat closed-box bridge deck. *Journal of Wind Engineering & Industrial Aerodynamics*, **122**(11):69-82.

Submitted: 01/11/2015

Revised : 12/11/2016

Accepted : 27/02/2017